JOURNAL OF COMPUTATIONAL PHYSICS **136,** 68–82 (1997)
ARTICLE NO. CP975742

A Domain Decomposition Method for the Helmholtz Equation and Related Optimal Control Problems

Jean-David Benamou,*,[1] and Bruno Desprès†,[2]

Domaine de Voluceau, INRIA, B. P. 105, 78153 Le Chesnay Cedex, France; and †Commissariat à l'Energie Atomique, 94195 Villeneuve Saint Georges Cedex, France

Received February 28, 1996; revised February 24, 1997

We present an iterative domain decomposition method to solve the Helmholtz equation and related optimal control problems. The proof of convergence of this method relies on energy techniques. This method leads to efficient algorithms for the numerical resolution of harmonic wave propagation problems in homogeneous and heterogeneous media.

1. INTRODUCTION

The numerical resolution of the Helmholtz equation and related optimal control problem in heterogeneous media at high wave number with various boundary conditions is a challenging problem. Domain Decomposition Methods (DDM) to solve some of these problems were developed in [3, 4, 7–9, 14–20, 29, 32, 38, 40]. These techniques can generally be extended to Maxwell's equations, which cover numerous applications in electromagnetics.

The aim of this paper is to give in a unified framework a formal presentation of the algorithm proposed in [15] for the exterior Helmholtz equation with the lowest order absorbing boundary condition and its extension to optimal control problems governed by this equation. We also present the application of this method to more general boundary conditions such as that arising in wave guide problems and to the heterogeneous case. We finally discuss the use of the DDM in conjunction with the PML technique [5].

The idea is to split the domain into smaller sub-domains and solve a sequence of similar sub-problems on these subdomains. The boundary conditions are adjusted iteratively by ad hoc transmission conditions between adjacent subdomains. The number and size of sub-domains can now be chosen to enable direct methods to solve the sub-problems. In the case of optimal control a classical technique requires the iterated resolution of direct and adjoint Helmholtz problems in order to compute descent directions for a gradient-type method. In this paper we decompose the coupled system composed by the direct and adjoint Helmholtz equation and the optimality condition which variationally expresses that the control is optimal. This method actually solves at the same time the equations and the optimization problem, whereas classical methods require the iterated resolution of direct and adjoint problems in order to compute descent directions for a gradient-type method. The proposed method is easy to implement and naturally adapted to parallel computers, the use of which is a major trend in modern scientific computing.

The main advantage of the DDM proposed in this paper, at least for the memory requirements of numerical simulations, is that it reduces the global problem to the iterative resolution of smaller sub-problems. The user is then free to choose any suitable existing Helmholtz volumic solver. Because they are designed for infinite domains, the use of standard integral methods [12, 33, 39] seems a priori impossible. They apply, moreover, only to the homogeneous case.

We present in Section 2 the domain decomposition method for the resolution of the exterior Helmholtz equation with the lowest order order boundary conditions. A proof of convergence is given based on energy estimates. We focus on these energy estimates since:

(i) These estimates are not standard in the context of elliptic coercive problems.

(ii) They help to understand why the algorithms converge.

(iii) Slight modifications of this technique can be used in various cases of boundary conditions and equations.

Section 3 deals with the optimal control of systems governed by such equations. Different "coupled" transmission conditions are introduced. Convergence is again obtained using energy estimates but the arguments differ from Section 2. Section 4 discusses the application of the domain decomposition to the inhomogeneous case, waveguides problems, and PML technique. A test case is solved numerically in Section 5.

[1] E-mail: Jean-David.Benamou@inria.fr.
[2] E-mail: despres@limeil.cea.fr.

0021-9991/97 $25.00

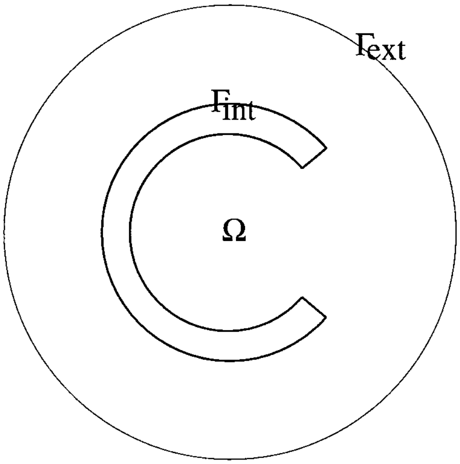

FIG. 1. Geometry of the diffraction problem: a resonator.

2. DDM FOR THE HELMHOLTZ PROBLEM

2.1. The Helmholtz Equation and the Truncated Domain

In this section we review the model and various boundary conditions for the exterior Helmholtz problem which will be considered throughout this paper.

Let Ω be a sufficiently smooth bounded open set in $\mathbb{R}^2$ or $\mathbb{R}^3$ containing an obstacle. The boundary $\Gamma = \partial\Omega$ is divided into an interior boundary Γ_{int} (the boundary of the resonator) and an exterior boundary Γ_{ext} (see Fig. 1. for example).

The out-going normal is denoted by ν. In a scattering problem the source term u_{inc}, called the incident wave (usually a plane wave), illuminates the object located inside Γ_{int}. The scattered wave is the complex valued solution of

$$\begin{cases} -\nabla(\mu\vec{\nabla}u) - \omega^2\rho u = f & \text{in } \Omega \\ \dfrac{\partial}{\partial\nu}u = -\dfrac{\partial}{\partial\nu}u_{\text{inc}} & \text{on } \Gamma_{\text{int}} \\ \dfrac{\partial}{\partial\nu}u + i\omega\sqrt{\dfrac{\rho}{\mu}} = 0 & \text{on } \Gamma_{\text{ext}}, \end{cases} \tag{1}$$

where ω is the frequency of the harmonic oscillations. The coefficients μ and ρ are strictly positive bounded, possibly discontinuous, real functions characterizing the non-dispersive medium. Their physical interpretation varies according to the modeled physical situation [39]. The source term f is given and arises from these inhomogeneities.

The boundary condition on Γ_{ext} is an absorbing boundary condition of the lowest order (following [1]). It approximates the outgoing character of the scattered wave on the truncated domain. In the exact model, the solution is defined in all space and satisfies the Sommerfeld radiation condition (expressed in polar coordinates, where r is the radius)

$$\frac{\partial}{\partial r}u + i\omega\sqrt{\frac{\rho}{\mu}} = O\left(\frac{1}{r^2}\right) \quad \text{when } r \text{ goes to } +\infty. \tag{2}$$

This approximate boundary condition is introduced to bound the domain for actual computations. We want to mention that this lowest order boundary condition on Γ_{ext} plays a fundamental role in the well-posedness of (1) (see [15, 26]) and in the design of the DDM presented in this paper. There exists of course more accurate absorbing boundary conditions. See, for instance, [1, 24] on this topic.

One may also want to use a non-local Dirichlet-to-Neumann operator (see [25, 27]) in the boundary conditions on Γ_{ext}. The boundary condition now takes the form

$$\frac{\partial}{\partial\nu}u + T(u) = 0. \tag{3}$$

This is the case in our wave-guide section (4.2.1).

The Neumann boundary condition imposed on Γ_{int} simulates the presence of a "hard" object. If one wants to study scattering by a "soft" object, one has to use a Dirichlet boundary condition $u = -u_{\text{inc}}$. Impedance boundary conditions

$$\frac{\partial}{\partial\nu}u + i\omega z u = -\frac{\partial}{\partial\nu}u_{\text{inc}} + i\omega z u_{\text{inc}}, \tag{4}$$

where z is a complex number, are also possible. $\text{Re}(z) \geq 0$ is a necessary condition to obtain well-posedness. This is a compatibility condition with the lowest order absorbing boundary condition. Impedance boundary condition can be derived from the Leontovitch boundary condition [6] for electromagnetic waves.

Finally let us mention the recent Perfectly Matched Layer technique [5], which consists in adding a damping layer around the computational domain. These PML are remarkable because they generate (for the continuous equations) no artificial reflections at the interface between the domain and the layers. Their numerical discretization and implementation for the Helmholtz equation have been studied with good results in [5, 10, 37]. We briefly describe these PML in a simplified situation. We consider the homogeneous (i.e., $u = \rho = 1$, $f = 0$) case in $\mathbb{R}^2$. Let (x, y) denote the space coordinates. Suppose we want to solve the problem in the half space $x < 0$. We extend the problem to the union of the half plane and an absorbing layer defined as a strip $0 < x < \delta$. In this case the PML has been shown to be equivalent in the layer to the modified equation [10, 11]

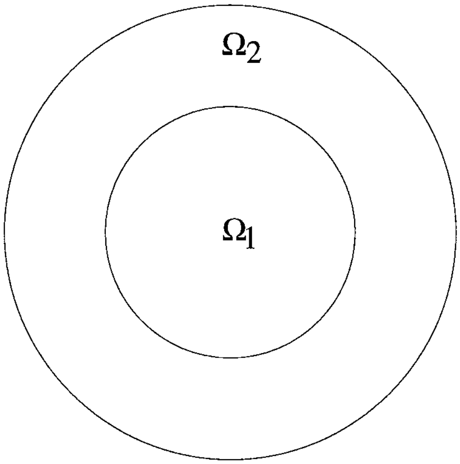

FIG. 2. Simple decomposition.

$$-\partial^2_{xx}u - d\partial_y(d\partial_y u) - \omega^2 u = 0, \tag{5}$$

where $d = i\omega/(i\omega + \sigma)$ and σ is a real parameter which is responsible for the exponential damping of the wave. The sign of σ determines the in-going/out-going character of the scattered wave.

2.2. The Domain Decomposition Method

We simplify the description of the method by restraining ourselves to the homogeneous case (i.e., $\mu = \rho = 1$, $f = 0$). The extension to the heterogeneous case is discussed in Section 4.1. The equation is now

$$\begin{cases} -\Delta u - \omega^2 u = 0 & \text{in } \Omega \\ \dfrac{\partial}{\partial \nu} u = -\dfrac{\partial}{\partial \nu} u_{\text{inc}} & \text{on } \Gamma_{\text{int}} \\ \dfrac{\partial}{\partial \nu} u + i\omega u = 0 & \text{on } \Gamma_{\text{ext}}. \end{cases} \tag{6}$$

2.2.1. *Transmission Conditions*

Let us consider a trivial case where Ω is split into 2 subdomains Ω_1 and Ω_2 such that the boundary of Ω_2 has an empty intersection with $\partial\Omega$ (see Fig. 2).

We denote by u_1 and u_2 the restrictions of u (solution of (6)) in respectively Ω_1 and Ω_2. u_1 and u_2 satisfy the interface conditions on $\partial\Omega_1 \cap \partial\Omega_2$

$$u_1 = u_2 \tag{7}$$

$$\frac{\partial}{\partial \nu_1} u_1 = -\frac{\partial}{\partial \nu_2} u_2, \tag{8}$$

where ν_i is the exterior normal to Ω_i. If $(\partial/\partial\nu_2)u_2$ is given, u_1 satisfy the equation $-\Delta u_1 - \omega^2 u_1 = 0$, with the boundary conditions (8) above.

It is well known, however, that this problem may be ill-posed due to the existence of eigenvalues of the Laplace operator [36]. We propose instead to linearly combine Eqs. (7) and (8) to get the equivalent boundary conditions

$$\frac{\partial}{\partial \nu_2} u_2 + i\omega u_2 = -\frac{\partial}{\partial \nu_1} u_1 + i\omega u_1 \tag{9}$$

and

$$\frac{\partial}{\partial \nu_1} u_1 + i\omega u_1 = -\frac{\partial}{\partial \nu_2} u_2 + i\omega u_2. \tag{10}$$

The sub-problem on Ω_1, together with condition (10), is now well posed. This sub-problem is of the same type as the global problem, which is well-posed thanks to the absorbing boundary condition (see above). These mixed (or "Robin") boundary conditions play an important role in the definition of our domain decomposition method.

2.2.2. *The Basic Algorithm*

We describe the domain decomposition algorithm. The idea is to adjust the boundary conditions iteratively at the interfaces between sub-domains to obtain transmission conditions of the type (9), (10).

We introduce some notations. Let us split Ω into a finite number of non-overlapping sub-domains Ω_k, $1 \leq k \leq K$, with sufficiently smooth boundaries. These sub-domains have interfaces denoted by $\Sigma_{kj} = \Sigma_{jk} = \partial\Omega_k \cap \partial\Omega_j$. They may also have a part of their boundaries impinging on Γ. So we write $\Gamma_{k,\text{ext}} = \partial\Omega_k \cap \Gamma_{\text{ext}}$ and $\Gamma_{k,\text{int}} = \partial\Omega_k \cap \Gamma_{\text{int}}$ (see Fig. 3). The out-going normal for Ω_k is ν_k.

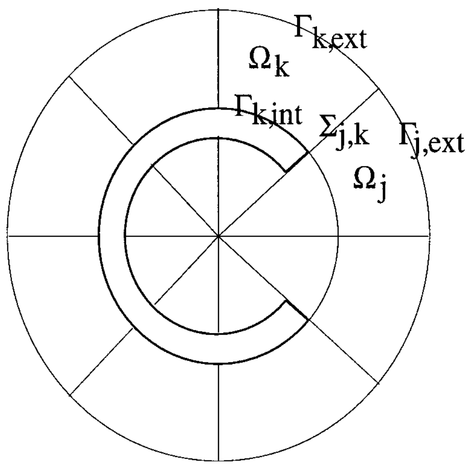

FIG. 3. A decomposition of the domain.

We now define the following iterative procedure using Robins transmission conditions (the superscript denotes the rank of the iterative procedure).

Initialize u_k^0 for all k, then iterate for $n > 0$

$$\begin{cases} -\Delta u_k^{n+1} - \omega^2 u_k^{n+1} = 0 & \text{in } \Omega_k \\ \dfrac{\partial}{\partial \nu_k} u_k^{n+1} + i\omega u_k^{n+1} = -\dfrac{\partial}{\partial \nu_j} u_j^n + i\omega u_j^n & \text{on } \Sigma_{kj} \\ \dfrac{\partial}{\partial \nu_k} u_k^{n+1} + i\omega u_k^{n+1} = 0 & \text{on } \Gamma_{k,\text{ext}} \\ \dfrac{\partial}{\partial \nu_k} u_k^{n+1} = \dfrac{\partial}{\partial \nu_k} u_{\text{inc}} & \text{on } \Gamma_{k,\text{int}}. \end{cases} \tag{11}$$

The boundary condition on $\Gamma_{k,\text{int}}$ for the sub-problems is determined according the boundary condition on Γ_{int} of the global problem (6) (i.e., $u_k^{n+1} = u_{\text{inc}}$ on $\Gamma_{k,\text{int}}$ for a soft obstacle and so forth). When $\Gamma_{k,\text{int}} = \emptyset$ or $\Gamma_{k,\text{ext}} = \emptyset$, i.e., Ω_k is an "interior" sub-domain, the corresponding boundary condition is simply ignored. This algorithm is an Helmholtz adaptation of the well-known Schwarz algorithm for elliptic problems described in [31]. Thanks to the Robin transmission conditions, the sub-problems are well posed. Notice that, at each step of the iterative procedure, the resolution of each sub-problem is explicit and independent of the other sub-problems.

2.2.3. *Convergence*

We are able to prove the convergence of the procedure (11) under various hypothesis on the regularity of the solution [15]. We do not want to go inside the mathematical details of the proof. We instead assume enough regularity on the global solution of (6) and of the initialization (u_k^0) of the iterative procedure to be able to define a "pseudo-energy" linked with the algorithm. Let us define the error

$$eu_k^n = u_k^n - u.$$

It satisfies equations (11) with $u_{\text{inc}} = 0$. The "pseudo-energy" at iteration n has the form ($|.|$ is the complex modulus)

$$E^n = \sum_{k \neq j} \int_{\Sigma_{kj}} \left(\left| \frac{\partial}{\partial \nu_k} eu_k^n \right|^2 + \omega^2 |eu_k^n|^2 \right) d\sigma. \tag{12}$$

We call that quantity a "pseudo-energy" because it is not a conventional energy. However, if $E^n = 0$, then both eu_k^n and $(\partial/\partial \nu_k) eu_k^n$ are equal to 0 on Σ_{kj}. This implies that (see [12]) $eu_k^n = 0$ in Ω_k.

The domain decomposition algorithm turns out to decrease this pseudo-energy. We have:

Proposition 1. *The pseudo-energy satisfies*

$$E^{n+1} = E^n - 2\omega^2 \sum_k \int_{\Gamma_{k,\text{ext}}} |eu_k^{n+1}|^2 + |eu_k^n|^2. \tag{13}$$

The proof comes from the following computations. First, using the equation on each sub-domain and integrating by parts against the conjugate of $i\omega eu_k^{n+1}$, we have

$$\begin{aligned} &\operatorname{Re}\left(\int_{\partial\Omega_k} \frac{\partial}{\partial \nu_k} eu_k^{n+1} \, \overline{i\omega eu_k^{n+1}} \, d\sigma \right) \\ &\quad = \operatorname{Re}\left(-i\omega \left(\int_{\Omega_k} |\nabla eu_k^{n+1}|^2 - \omega^2 |eu_k^{n+1}|^2 \right) dx \right) = 0. \end{aligned} \tag{14}$$

Then, using the boundary conditions on $\Gamma_{k,\text{int}}$, $\Gamma_{k,\text{ext}}$, we recombine in (13) the integral on the boundary of each sub-domain to express the missing cross products in (15):

$$\begin{aligned} E^{n+1} = &\sum_{k \neq j} \int_{\Sigma_{kj}} \left| \frac{\partial}{\partial \nu_k} eu_k^{n+1} + i\omega eu_k^{n+1} \right|^2 d\sigma \\ &- 2\omega^2 \sum_k \int_{\partial\Gamma_{k,\text{ext}}} |eu_k^{n+1}|^2 \, d\sigma. \end{aligned} \tag{15}$$

The transmission conditions now give

$$\begin{aligned} E^{n+1} = &\sum_{k \neq j} \int_{\Sigma_{kj}} \left| -\frac{\partial}{\partial \nu_k} eu_k^n + i\omega eu_k^n \right|^2 d\sigma \\ &- 2\omega^2 \sum_k \int_{\partial\Gamma_{k,\text{ext}}} |eu_k^{n+1}|^2 \, d\sigma. \end{aligned} \tag{16}$$

We finally use the analog of (14) at step n to obtain (13).

We deduce from Proposition 1 that:

(i) (E^n) is a bounded sequence.

(ii) $\sum_k \int_{\Gamma_{k,\text{ext}}} |eu_k^n|^2 \, d\sigma$ goes to 0 as the generic term of a convergent series.

This is enough to prove the convergence of the domain decomposition method. We establish that the error is null in the sub-domain bordering Γ_{ext} and show the same property for the interior sub-domain by an iterative progression.

The convergence theorem is (see [15]):

Theorem 1. *For all* k, *we have*

$$\int_{\Omega_k} |\nabla u_k^n - \nabla u|^2 + |u_k^n - u|^2 \, dx \text{ goes to } 0 \text{ with } n.$$

We want here to point out the importance of the first order absorbing condition in the convergence process. It is used in the proof to obtain the quantity

$\sum_k \int_{\Gamma_{k,\text{ext}}} |eu_k^n|^2\, d\sigma$ on the right hand side of (13), which decreases the pseudo-energy of the error.

An impedance boundary condition on Γ_{int} (4) will turn this term into $-\text{Re}(z)\int_{\Gamma_{k,\text{int}}} |eu_k^n|^2\, d\sigma$. Hence the importance of the sign of z stressed in section 2.1.

An other choice of boundary condition on Γ_{ext} such as a higher order absorbing boundary condition or a non-local operator T as in (3) does not allow to prove convergence of the algorithm. This point is discussed in Section 4.2.

2.2.4. *Under-Relaxation*

A slight modification of the basic algorithm generates a new algorithm which has a much better rate of convergence in applications [16]. We call it the under-relaxed algorithm because of the introduction of a real parameter $r \in]0., 0.5[$ which can be viewed as a relaxation parameter.

It simply consists in the following modification of the transmission condition in (11):

$$\begin{aligned} \frac{\partial}{\partial \nu_k} u_k^{n+1} + i\omega u_k^{n+1} &= (1-r)\left(-\frac{\partial}{\partial \nu_j} u_j^n + i\omega u_j^n\right) \\ &\quad + r\left(\frac{\partial}{\partial \nu_k} u_k^n + i\omega u_k^n\right) \quad on\ \Sigma_{kj}. \end{aligned} \tag{17}$$

We find (after some computations) that the new law for the decrease of the pseudo-energy (12) is now given by

$$\begin{aligned} E^{n+1} = E^n - 2\omega^2 &\left(\sum_k \int_{\Gamma_{k,\text{ext}}} |eu_k^{n+1}|^2\, d\sigma \right. \\ &\left. - (1-2r)\int_{\Gamma_{k,\text{ext}}} |eu_k^n|^2\, d\sigma\right) \\ &- 2r(1-r)\left(\sum_{k,j}\int_{\Sigma_{kj}} \left|\frac{\partial}{\partial \nu_k} eu_k^n \right.\right. \\ &\left.\left. + \frac{\partial}{\partial \nu_j} eu_j^n\right|^2 + \omega^2 |eu_k^n - eu_j^n|^2\, d\sigma\right). \end{aligned} \tag{18}$$

In addition to the usual norm of the error on the external boundaries $\Gamma_{k,\text{ext}}$ (first line of (18)), the pseudo-energy is decreased by a new factor which depends on the relaxation parameter (second line). This new quantity turns out to be a norm of the error [15]. Indeed, if this term is null, the error satisfies a Helmholtz equation on the whole domain with homogeneous boundary condition. This implies that the error is zero everywhere.

The same modification of the transmission condition and remark on the behavior of the under-relaxed algorithm also hold for the optimal control case (Section 3).

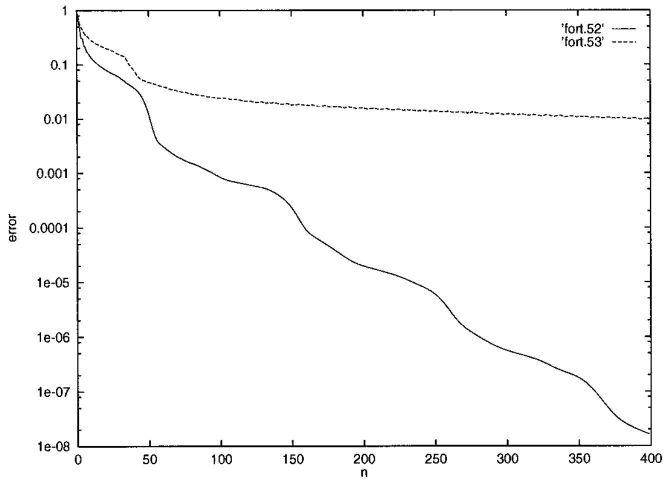

FIG. 4. Convergence history. Dashed line: standard algorithm; solid line: under-relaxed algorithm.

2.2.5. *Numerical Rate of Convergence*

We illustrate the theoretical results of convergence with two simple numerical experiments (also described in [16]).

In a first experiment we consider a slightly different problem than in (6) where there is no scatterer but a source point at the center of the domain. The solution u satisfies

$$\begin{cases} (-\Delta - \omega^2)u = \delta & \text{in } \Omega, \\ \left(\dfrac{\partial}{\partial \nu} + i\omega\right) u = 0 & \text{on } \Gamma_{\text{ext}}. \end{cases} \tag{19}$$

We take $\omega = 2\pi$ such that the wavelength is 1. The solution u is made of radial oscillations which approximate the fundamental out-going solution $H_0^{(2)}/4i$ of the Helmholtz equation in the plane. The domain is $\Omega = [-9.75, 9.75] \times [-9.75, 9.75]$, and sub-domains are rectangles of size 1.3×0.3. There are 975 rectangular subdomains. The mesh size is $h = 0.1$, so there are 195^2 cells in the mesh. We use a finite element technique [15, 22] combined with an exact inversion of the linear systems arising from the local sub-problems.

The relative error $\|u^n - u^{n+1}\|_{L^2(\Omega)}/\|u^{n+1}\|_{L^2(\Omega)}$ is plotted versus the number of iterations of the DDM. We obtain (Fig. 4) a convergence history which shows that the under-relaxed algorithm for $r = 0.3$ converges much better than the basic algorithm.

A much more difficult case, from the convergence point of view, is (still with a source point at the center of the domain)

$$\begin{cases} (-\Delta - \omega^2)u = \delta & \text{in } \Omega, \\ \left(\dfrac{\partial}{\partial \nu} + i\omega z\right) u = 0 & \text{on } \Gamma_{\text{ext}}. \end{cases} \tag{20}$$

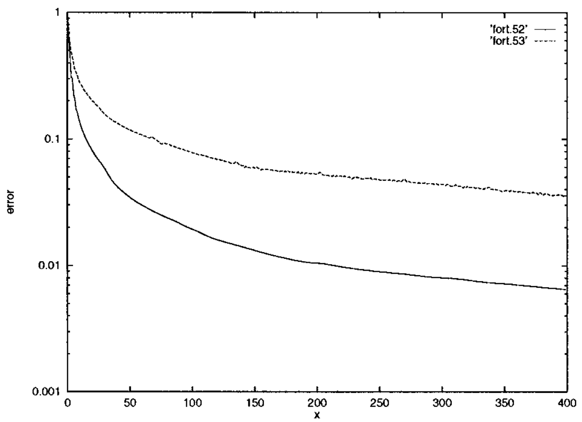

FIG. 5. Convergence history. Dashed line: standard algorithm; solid line: under-relaxed algorithm.

where the impedance z takes the values

$$z = 0, 1 + 2i, 0, 2 + i,$$

respectively on the right, top, left, bottom edges of the square. With the same domain decomposition, we obtain the following convergence history (Fig. 5), which again shows that the under-relaxed algorithm still converges better than the basic algorithm. The convergence is not as good as in the case $z = 1$ everywhere. This is due to multiple reflections on the boundaries mostly produced by the Neumann boundary conditions on the left and right boundaries.

3. DDM FOR OPTIMAL CONTROL

3.1. The Optimal Control Problem

We consider the problem of the optimal control of a system governed by the Helmholtz problem (6) of Section 3.

The boundary Γ_{int} of the scattering obstacle is now split into two parts (see Fig. 6).

On one part, we have the previous scattering boundary condition; this is still denoted Γ_{int}. A second part, called Γ_{ctr}, is the interior boundary of the scatterer (between dots on Fig. 6) on which we had a control variable v, a complex value function, in the boundary condition:

$$\frac{\partial}{\partial\nu}u = -\frac{\partial}{\partial\nu}u_{\text{inc}} + v \quad on\,\Gamma_{\text{ctr}}. \tag{21}$$

The solution $u(v)$ of the scattering problem (6) (21) now depends on the control v, which models artificial emission of surface currents for electromagnetic waves or forced vibration for acoustic waves.

We want to solve the optimization problem

$$\min_{v\in U} J(u(v), v), \tag{22}$$

where U is a closed convex set of admissible controls and J a given cost functional.

The simplest example of such a cost function is given by

$$J(u, v) = \left\{\int_\Omega \frac{1}{2}|u|^2\,dx + \frac{\alpha}{2}\int_{\Gamma_{\text{ctr}}} |v|^2\,d\sigma\right\}, \tag{23}$$

where α is a strictly positive penalization parameter. The first part of the above functional is a norm of the scattered field. We try to make the scatterer invisible to the probing incident plane wave. The penalization part takes into account the norm of the control. Adjusting the penalization parameter α, we can make a compromise between the minimization of the energy of the scattered field and the cost of this minimization. As we only control a part of the boundary of the scattering object and because of the penalization term, the solution is not trivially $v = -u_{\text{inc}}$.

Thanks to the strict convexity of the functional, the optimization problem has a unique solution. It is characterized by the adjoint problem

$$\begin{cases} -\Delta p - \omega^2 p = u & \text{in } \Omega \\ \dfrac{\partial}{\partial\nu}p = 0 & \text{on } \Gamma_{\text{int}} \cup \Gamma_{\text{ctr}} \\ \dfrac{\partial}{\partial\nu}p - i\omega p = 0 & \text{on } \Gamma_{\text{ext}} \end{cases} \tag{24}$$

and the optimality condition

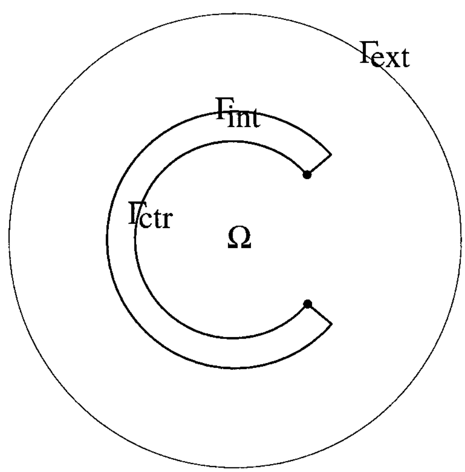

FIG. 6. New decomposition of the boundary of the scatterer.

$$\int_{\Gamma_{\mathrm{ctr}}} \mathrm{Re}((p + \alpha v)(\overline{w - v}))\, d\sigma \geq 0, \quad \forall w \in U, \tag{25}$$

which provide a variational expression of the gradient of the functional. For more general formulations of optimal control problems see [30].

3.2. The Domain Decomposition Method

We present in this section the application of the domain decomposition algorithm to the resolution of the coupled system (6), (21), (24), (25).

3.2.1. *The Iterative Algorithm*

The domain Ω is decomposed as in Section 2.2. We keep the same notations and add $\Gamma_{k,\mathrm{ctr}} = \partial\Omega_k \cap \Gamma_{\mathrm{ctr}}$.

We define a family (U_k) of closed convex sets of admissible local controls on each $\Gamma_{k,\mathrm{ctr}}$ satisfying compatibility conditions with U:

$$\begin{aligned} &\forall v \in U, v|_{\Gamma_{k,\mathrm{ctr}}} \in U_k \quad \text{and} \\ &\forall v_k \in U_k, v, \text{such that } v|_{\Gamma_{k,\mathrm{ctr}}} = v_k\ \forall k, \text{belongs to } U. \end{aligned} \tag{26}$$

These conditions are satisfied by the usual local constraints on the control variable. A typical example is

$$\begin{aligned} &U = \{v, \xi_0(x) \leq v(x) \leq \xi_1(x) \text{ for a.e. } x \in \Gamma_{\mathrm{ctr}}\}\ \textit{and} \\ &U_k = \{v_k, \xi_0(x) \leq v_k(x) \leq \xi_1(x) \text{ for a.e. } x \in \Gamma_{k,\mathrm{ctr}}\} \\ &\xi_0, \xi_1 \in L^\infty(\Gamma_{\mathrm{ctr}}); \end{aligned}$$

conversely, global or state constraints do not a priori satisfy (26).

We now describe the method, as in Section 2.2.

Initialize u_k^0, p_k^0 for all k, then iterate for $n > 0$:

$$\begin{cases} -\Delta u_k^{n+1} - \omega^2 u_k^{n+1} = 0 & \text{in } \Omega_k \\ \dfrac{\partial}{\partial \nu_k} u_k^{n+1} + i\omega u_k^{n+1} = 0 & \text{on } \Gamma_{k,\mathrm{ext}} \\ \dfrac{\partial}{\partial \nu_k} u_k^{n+1} = \dfrac{\partial}{\partial \nu_k} u_{\mathrm{inc}} & \text{on } \Gamma_{k,\mathrm{int}} \\ \dfrac{\partial}{\partial \nu_k} u_k^{n+1} = \dfrac{\partial}{\partial \nu_k} u_{\mathrm{inc}} + v_k^{n+1} & \text{on } \Gamma_{k,\mathrm{ctr}} \end{cases} \tag{27}$$

$$\begin{cases} -\Delta p_k^{n+1} - \omega^2 p_k^{n+1} = u_k^{n+1} & \text{in } \Omega_k \\ \dfrac{\partial}{\partial \nu_k} p_k^{n+1} - i\omega p_k^{n+1} = 0 & \text{on } \Gamma_{k,\mathrm{ext}} \\ \dfrac{\partial}{\partial \nu_k} p_k^{n+1} = 0 & \text{on } \Gamma_{k,\mathrm{int}} \cup \Gamma_{k,\mathrm{ctr}} \end{cases} \tag{28}$$

$$\begin{aligned} \int_{\Gamma_{k,\mathrm{ctr}}} &\mathrm{Re}((p_k^{n+1} + \alpha v_k^{n+1})(\overline{w_k - v_k^{n+1}}))\, d\sigma \\ &\geq 0, \quad \forall w_k \in U_k. \end{aligned} \tag{29}$$

These sub-problems are simply the restrictions of our original problem to the sub-domains. The unknowns are u_k^{n+1}, p_k^{n+1}, and a local control variable v_k^{n+1} for the sub-domains bordering the control boundary, i.e., such that $\Gamma_{k,\mathrm{ctr}} \neq \emptyset$.

We need to specify the transmission conditions on the interfaces Σ_{kj} between sub-domains in order to ensure that the sequence of local solutions of these sub-problems converges to the solution of the global problem.

3.2.2. *The Transmission Conditions*

For the Helmholtz equation we used transmission conditions in the form of Robin boundary conditions:

$$\frac{\partial}{\partial \nu_k} u_k^{n+1} + i\omega u_k^{n+1} = -\frac{\partial}{\partial \nu_j} u_j^n + i\omega u_j^n.$$

If we try to apply the same transmission conditions to the direct and adjoint equation, which are both Helmholtz equations, i.e.,

$$\frac{\partial}{\partial \nu_k} p_k^{n+1} + i\omega p_k^{n+1} = -\frac{\partial}{\partial \nu_j} p_j^n + i\omega p_j^n,$$

we cannot prove the convergence of the algorithm, the reason being the coupling between the direct, adjoint, and control variables in the equations.

This same coupling suggested the introduction of coupled transmission conditions in [4] for the optimal control of systems governed by scalar elliptic equations. We show here that this is also a suitable choice in the case of systems governed by the Helmholtz equation. The coupled transmission conditions take the form

$$\begin{aligned} &\frac{\partial}{\partial \nu_k} u_k^{n+1} + \lambda p_k^{n+1} = -\frac{\partial}{\partial \nu_j} u_j^n + \lambda p_j^n\ \textit{on}\ \Sigma_{kj}, \\ &\frac{\partial}{\partial \nu_k} p_k^{n+1} - \lambda u_k^{n+1} = -\frac{\partial}{\partial \nu_j} p_j^n - \lambda u_j^n\ \textit{on}\ \sigma_{kj}, \end{aligned} \tag{30}$$

with λ a real positive parameter.

3.2.3. *Decomposition in Local Optimal Control Problems*

The algorithm (27), (28), (30), (29) is now well defined; i.e., it can be shown that the sub-problems are well posed. They can actually be reinterpreted as the minimization of $J_k(\tilde{v}_k)$,

$$J_k(\tilde{v}_k) = \int_{\Omega_k} \frac{1}{2}|\tilde{u}_k|^2\,dx + \int_{\Gamma_{k,\mathrm{ctr}}} \frac{\alpha}{2}|\tilde{v}_k|^2\,d\sigma + \sum_j \int_{\Sigma_{kj}} \frac{\lambda}{2}\left(\left|\frac{\partial}{\partial \nu_k}\tilde{p}_k\right|^2 + |\tilde{p}_k|^2\right) d\sigma, \tag{31}$$

where $\tilde{u}_k, \tilde{p}_k$ are functions of $\tilde{v}_k$ and solution of the coupled sub-problems (27), (28), (30) with $\tilde{u}_k$, $\tilde{p}_k$, $\tilde{v}_k$, instead of u_k^{n+1}, p_k^{n+1}, v_k^{n+1}. This functional is of course only defined for sub-domains Ω_k such that $\Gamma_{k,\mathrm{ctr}} \neq \emptyset$. The other sub-problems simply consist of two coupled Helmholtz equations and involve no control variable.

The optimality condition for the minimization of the functional J_k can be written

$$J'_k(\tilde{v}_k)\cdot(w_k - \tilde{v}_k) \geq 0, \quad \forall w_k \in U_k, \tag{32}$$

where $\tilde{v}_k$ is the optimal control.

Let us define $\delta v_k = w_k - \tilde{v}_k$. We denote by $(\delta u_k, \delta p_k)$ (functions of δv_k) the solution of the linear equations (27), (28), (30) with δu_k, δp_k, δv_k instead of $u_k^{n+1}, p_k^{n+1}, v_k^{n+1}$ and with every source term set to 0.

With these notations (32) may be rewritten as

$$\int_{\Omega_k} \mathrm{Re}(\tilde{u}_k, \overline{\delta u_k})\,dx + \alpha\int_{\Gamma_{k,\mathrm{ctr}}} \mathrm{Re}(\tilde{v}_k, \overline{\delta v_k})\,d\sigma + \sum_k \lambda \int_{\Sigma_{kj}} \mathrm{Re}\left(\frac{\partial}{\partial \nu_k}\tilde{p}_k, \frac{\partial}{\partial \nu_k}\overline{\delta p_k}\right) + \mathrm{Re}(\tilde{p}_k, \overline{\delta p_k})\,d\sigma \geq 0, \quad \forall \delta v_k \in U_k - \tilde{v}_k. \tag{33}$$

On the other hand, using the Green formula

$$\int_{\Omega_k} (\Delta\tilde{p}_k, \overline{\delta u_k}) - (\Delta\overline{\delta u_k}, \tilde{p}_k)\,dx = \int_{\partial\Omega_k}\left(\frac{\partial}{\partial \nu_k}\tilde{p}_k, \overline{\delta u_k}\right) - \left(\frac{\partial}{\partial \nu_k}\overline{\delta u_k}, \tilde{p}_k\right) d\sigma \tag{34}$$

and the equations (27), (28), (30), we obtain

$$\int_{\Gamma_{k,\mathrm{ctr}}} (\tilde{p}_k, \overline{\delta v_k})\,d\sigma = \int_{\Omega_k} (\tilde{u}_k, \overline{\delta u_k})\,dx + \sum_k \lambda \int_{\Sigma_{kj}} \left(\frac{\partial}{\partial \nu_k}\tilde{p}_k, \frac{\partial}{\partial \nu_k}\overline{\delta p_k}\right) + (\tilde{p}_k, \overline{\delta p_k})\,d\sigma. \tag{35}$$

Taking the real part of the above quantity, we see that (33), (35) reduce to

$$\int_{\Gamma_{k,\mathrm{ctr}}} \mathrm{Re}(\tilde{p}_k + \alpha\tilde{v}_k, \overline{w_k - \tilde{v}_k})\,d\sigma \geq 0\ \forall w_k \in U_k.$$

We recognize (29). Therefore, $\tilde{u}_k$, $\tilde{p}_k$, $\tilde{v}_k$ solve the sub-problem (27), (28), (30), (29) and $(\tilde{u}_k, \tilde{p}_k, \tilde{v}_k) = (u_k^{n+1}, p_k^{n+1}, v_k^{n+1})$. This sub-problem is equivalent to the minimization of J_k given above.

This local cost function is composed of two terms. One term is simply the restriction of the original global cost function to the considered sub-domain. The other term arises because of the coupling introduced in the transmission conditions (30). It aims at minimizing the Neumann and Dirichlet boundary values of p_k^{n+1}. This makes sense as we intend p_k^{n+1} to converge to p on Ω_k and therefore to the smallest possible value as p provide an expression of the gradient of $\int_\Omega \frac{1}{2}|u(v)|^2\,dx$, the scattering term of our cost function J.

This interpretation is only valid for the particular form of the cost function (23) and for the sub-domains on which a control is applied. In a boundary and observation control case, for example the one described in Section 3.2.5, where we use the functional (43), the observation $u(v)$ will act on the sub-domains bordering Γ_{ext} while the control will be split on the sub-domains satisfying $\Gamma_{k,\mathrm{ctr}} \neq \emptyset$. The geometrical domain decomposition may be such that these two class of sub-domains have an empty intersection in which case the first term of the functional (31) disappear. It is natural to believe that such a decomposition will have some influence on the rate of convergence.

We finally note that whatever the problem, the optimization process will be restricted to the sub-domains with non empty intersection with the support of the control variable. The number of degrees of freedom on which an actual optiization will be performed can therefore be greatly reduced compared to the global optimal control problem.

3.2.4. *The Convergence Result*

Let (u, p, v) denote the solution of the global optimal control problem (6), (21), (24), (25). We define the errors of our approximate sequence with the exact solution by

$$eu_k^n = u_k^n - u, ep_k^n = p_k^n - p, ev_k^n = v_k^n - v.$$

These errors satisfy the linear equations (27), (28), (30), (29) with $u_{\mathrm{inc}} = 0$.

Using (25), (29) and the compatibility conditions (26), we obtain the estimate (just subtract)

$$-\int_{\Gamma_{k,\mathrm{ctr}}} |ev_k^{n+1}|^2\,d\sigma \geq \int_{\Gamma_{k,\mathrm{ctr}}} \mathrm{Re}(ep_k^{n+1}\overline{ev_k^{n+1}})\,d\sigma \tag{36}$$

which is to be used in the proof of convergence.

As in Section 2.2.3, we define a pseudo-energy

$$E^{n+1} = \sum_{k\neq j} \int_{\Sigma_{kj}} \left| \frac{\partial}{\partial \nu_k} eu_k^{n+1} \right|^2 + \lambda^2 |eu_k^{n+1}|^2 + \left| \frac{\partial}{\partial \nu_k} ep_k^{n+1} \right|^2 + \lambda^2 |ep_k^{n+1}|^2 \, d\sigma. \tag{37}$$

This is a natural extension of (13).

The domain decomposition algorithm decreases this pseudo-energy. We have

PROPOSITION 2. *The pseudo-energy satisfies*

$$E^{n+1} \leq E^n - \lambda \sum_k \left(\int_{\Omega_k} |eu_k^{n+1}|^2 \, dx + \int_{\Gamma_{k,\text{ctr}}} |ev_k^{n+1}|^2 \, d\sigma + \int_{\Omega_k} |eu_k^n|^2 \, dx + \int_{\Gamma_{k,\text{ctr}}} |ev_k^n|^2 \, d\sigma \right). \tag{38}$$

Let us proceed to the proof of this proposition. Using the equation on the errors, we obtain

$$\begin{aligned} \text{Re} &\left(\int_{\partial\Omega_k} \frac{\partial}{\partial \nu_k} ep_k^{n+1} \overline{\lambda eu_k^{n+1}} - \frac{\partial}{\partial \nu_k} eu_k^{n+1} \overline{\lambda ep_k^{n+1}} \, d\sigma \right) \\ &= \text{Re} \left(\lambda \int_{\Omega_k} \nabla ep_k^{n+1} \overline{\nabla eu_k^{n+1}} - \nabla eu_k^{n+1} \overline{\nabla ep_k^{n+1}} \right. \\ &\quad \left. + \omega^2 (ep_k^{n+1} \overline{eu_k^{n+1}} - eu_k^{n+1} \overline{ep_k^{n+1}} \, dx \right) \\ &\quad + \lambda \int_{\Omega_k} |eu_k^{n+1}|^2 \, dx. \\ &= \lambda \int_{\Omega_k} |eu_k^{n+1}|^2 \, dx. \end{aligned} \tag{39}$$

Note that the terms which vanish on the right hand side of this equality do so precisely because u and p solve adjoint equations. Using thew boundary conditions on $\Gamma_{k,\text{int}}$ and $\Gamma_{k,\text{ctr}}$ and $\Gamma_{k,\text{int}}$, we substitute the left hand side of (39). The boundary terms on Γ_{int} and Γ_{ext} again vanish because of the adjointness of the boundary conditions. This is a general feature of the algorithm which will prove useful in different situations (see also Section 4.2).

$$\begin{aligned} \text{Re} &\left(\sum_j \int_{\Sigma_{kj}} \frac{\partial}{\partial \nu_k} ep_k^{n+1} \overline{\lambda eu_k^{n+1}} - \frac{\partial}{\partial \nu_k} eu_k^{n+1} \overline{\lambda ep_k^{n+1}} \, d\sigma \right) \\ &= \text{Re} \left(\lambda \int_{\Gamma_{k,\text{ext}}} i (ep_k^{n+1} \overline{eu_k^{n+1}} + eu_k^{n+1} \overline{ep_k^{n+1}} \, d\sigma \right) \\ &\quad + \lambda \int_{\Omega_k} |eu_k^{n+1}|^2 \, dx + \text{Re} \left(\lambda \int_{\Gamma_{k,\text{ctr}}} ep_k^{n+1} \overline{eu_k^{n+1}} \, d\sigma \right) \\ &= \lambda \int_{\Omega_k} |eu_k^{n+1}|^2 \, dx - \text{Re} \left(\lambda \int_{\Gamma_{k,\text{ctr}}} ep_k^{n+1} \overline{ev_k^{n+1}} \, d\sigma \right). \end{aligned} \tag{40}$$

We can now rewrite the pseudo-energy,

$$\begin{aligned} E^{n+1} &= \sum_{k\neq j} \int_{\Sigma_{kj}} \left| \frac{\partial}{\partial \nu_k} eu_k^{n+1} - \lambda ep_k^{n+1} \right|^2 \\ &\quad + \left| \frac{\partial}{\partial \nu_k} ep_k^{n+1} + \lambda ep_k^{n+1} \right|^2 d\sigma \\ &\quad + \sum_k \left(\text{Re} \left(\lambda \int_{\Gamma_{k,\text{ctr}}} ep_k^{n+1} \overline{ev_k^{n+1}} \, d\sigma \right) \right. \\ &\quad \left. - \lambda \int_{\Omega_k} |eu_k^{n+1}|^2 \, dx \right). \end{aligned}$$

The transmission conditions (30) and an equation at step n similar to (40) give

$$\begin{aligned} E^{n+1} = E^n + \sum_k &\left(\text{Re} \left(\lambda \int_{\Gamma_{k,\text{ctr}}} ep_k^{n+1} \overline{ev_k^{n+1}} \, d\sigma \right) \right. \\ &- \lambda \int_{\Omega_k} |eu_k^{n+1}|^2 \, dx + \text{Re} \left(\lambda \int_{\Gamma_{k,\text{ctr}}} ep_k^{n+1} \overline{ev_k^{n+1}} \, d\sigma \right) \\ &\left. - \lambda \int_{\Omega_k} |eu_k^{n+1}|^2 \, dx \right) \end{aligned}$$

It is time to use the optimality conditions (36). Substituting into the above expression, we finally prove (38). It can be straightforwardly deduced that

(i) (E^n) is a bounded sequence.

(ii) $\sum_k \int_{\Omega_k} |eu_k^n|^2 \, dx$ goes to 0 as the generic term of a convergent series.

(iii) $\sum_k \int_{\Gamma_{k,\text{ctr}}} |ev_k^n|^2 \, d\sigma$ goes to 0 as the generic term of a convergent series.

The convergence theorem now is

THEOREM 2. *For all k, the following quantities*

$$\int_{\Omega_k} |\nabla u_k^n - \nabla u|^2 + |u_k^n - u|^2 \, dx,$$

$$\int_{\Omega_k} |\nabla p_k^n - \nabla p|^2 + |p_k^n - p|^2 \, dx,$$

$$\int_{\Gamma_{k,\text{ctr}}} |v_k^n - v|^2 \, d\sigma,$$

go to 0 *with* n.

The proof, relying on (i), (ii), (iii) is similar to the proof of Theorem 1 detailed in [15] (see also [4]).

The interested reader will actually see by making the computations himself that the classical Robin boundary condition of Section 2 cannot yield the same convergence result (because of the coupling).

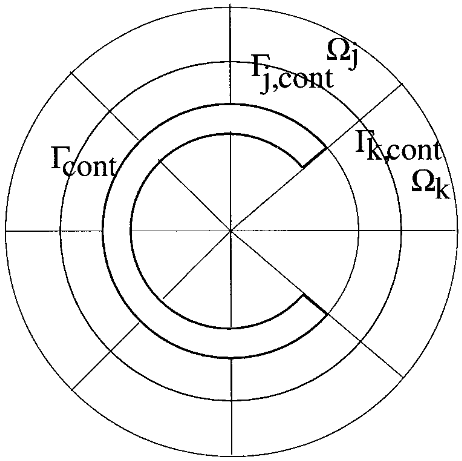

FIG. 7. Decomposition of the contour.

Inequation (38) indicates a different behavior of the algorithm for the optimal control problem compared to (13) for the plan Helmholtz problem. The decrease of the pseudo-energy does not depend any longer on the boundary condition or even on differential operator used in the direct problem but only on the second hand term of the adjoint equation. This will prove useful in Section 5.2, where we discuss different problems and boundary conditions.

3.3. Minimization of the Far Field

The above method applies to a wide class of linear optimal control problems (see [30] for a review of such problems).

We focus in this section to the case of a non-local cost function involving the expression of the far field (used to define the radar cross section), which turns out to be more interesting from the application point of view.

Let us assume that u has the following asymptotic expansion at infinity in polar coordinates:

$$u(r,\theta) = \frac{e^{-i\omega r}}{r^{1/2}}\{C(u,\theta) + O(r^{-1})\}. \tag{41}$$

$C(u, \theta)$ is the far field in the direction θ and this equation is equivalent to (2). Let us take Γ_{cont} to be a contour surface containing the scattering obstacle (see Fig. 7). A classical result of integral equation theory [13, p. 66] gives

$$C(u,\theta) = \frac{e^{-i}\pi/4}{\sqrt{8\pi\omega}}\int_{\Gamma_{\mathrm{cont}}} \times\left(-\frac{\partial}{\partial\nu}u(M) + i\omega\boldsymbol{\nu}\cdot\mathbf{d}u(M)\right)e^{i\omega \vec{OM}\cdot\mathbf{d}}\,d\sigma(M).$$

where $\boldsymbol{\nu}$ is the exterior normal at a point M running on Γ_{cont} and $\mathbf{d} = (\cos(\theta), \sin(\theta))$.

We take as a cost function

$$J(u(v),v) = \left\{\int_A \frac{1}{2}|C(u(v),\theta)|^2\,d\theta + \frac{\alpha}{2}\int_{\Gamma_{\mathrm{ctr}}}|v|^2\,d\sigma\right\}, \tag{42}$$

where, in 2-D, A is a given angular sector, subset of $[0, 2\pi[$.

The expansion (41) indicates, in the case when $A = [0, 2\pi[$, that an approximation of the cost function (42) is given by

$$J(u(v),v) = \left\{\int_{\Gamma_{\mathrm{ext}}} \frac{1}{2}|(u(v)|^2\,d\sigma + \frac{\alpha}{2}\int_{\Gamma_{\mathrm{ctr}}}|v|^2\,d\sigma\right\} \tag{43}$$

where the integration is performed on the exterior boundary Γ_{ext} (taken here as a circle of diameter 1).

The adjoint equation, analog of (24) for that particular cost function (43), is now

$$\begin{cases} -\Delta p - \omega^2 p = 0 & \text{in } \Omega \\ \dfrac{\partial}{\partial\nu}p = 0 & \text{on } \Gamma_{\mathrm{int}} \cup \Gamma_{\mathrm{ctr}} \\ \dfrac{\partial}{\partial\nu}p - i\omega p = u & \text{on } \Gamma_{\mathrm{ext}}. \end{cases}$$

The optimality condition (25) is unchanged and the domain decomposition and proof of convergence easily adopted.

If we decide to keep the exact formulation of the far field as given in (42), the adjoint equation is now

$$\begin{cases} -\Delta p - \omega^2 p = C^*(C(u)) & \text{in } \Omega \\ \dfrac{\partial}{\partial\nu}p = 0 & \text{on } \Gamma_{\mathrm{int}} \cup \Gamma_{\mathrm{ctr}} \\ \dfrac{\partial}{\partial\nu}p - i\omega p = 0 & \text{on } \Gamma_{\mathrm{ext}}, \end{cases}$$

where C^* is the adjoint operator of C and the optimality condition (25) is still unchanged. A mathematical study of existence and uniqueness of solutions for such a problem can be found in [23].

We now discuss the application of our algorithm to this problem. We modify accordingly our algorithm and (28) becomes

$$-\Delta p_k^{n+1} - \omega^2 p_k^{n+1} = C^*(C(u_{\mathrm{cont}}^{n+1}))\text{ in }\Omega_k, \tag{44}$$

where for all k, $u_{\text{cont}}^{n+1} = u_k^{n+1}$ on $\Gamma_{k,\text{cont}}$ with the obvious notation $\Gamma_{k,\text{cont}} = \partial\Omega_k \cap \Gamma_{\text{cont}}$ (see Fig. 7).

Convergence of the algorithm with the same coupled transmission condition (30) can be proved using the same kind of arguments.

Due to the non-local character of the functional C we see that the resolution of the sub-problems set in sub-domains having non-empty intersection with Γ_{cont} is no longer explicit. These sub-problems are instead coupled through the right hand side of equation (44). A simple solution to this problem is of course to decompose the domain Ω such that Γ_{cont} be fully contained in only one sub-domain.

One could also try to relax the coupling term by replacing it by $C^*(C(u_{\text{cont}}^n))$ which is available from the previous iteration. In this case, we cannot prove convergence.

3.4. Using the Optimal Control Algorithm to Solve the Plain Direct Problem

In this section we explain how the Optimal Control algorithm can be used to solve the plain direct Helmholtz problem.

We first remark that we can add a fictive adjoint problem to the direct scattering problem. Instead of solving simply (6) we also consider the problem

$$\begin{cases} -\Delta p - \omega^2 p = u & \text{in } \Omega \\ \dfrac{\partial}{\partial \nu} p = 0 & \text{on } \Gamma_{\text{int}} \cup \Gamma_{\text{ctr}} \\ \dfrac{\partial}{\partial \nu} p - i\omega p = 0 & \text{on } \Gamma_{\text{ext}}. \end{cases} \tag{45}$$

The adjoint problem is well posed and depends on u. It is similar to the optimal control problem of Section 4 except for the absence of control variable v and optimality condition (25).

We now apply the domain decomposition (27) (28) (30) of Section 4 where we forget the control variable v_k^{n+1} (i.e., we systematically take $v_k^{n+1} = 0$) and the optimality condition (29) to solve the coupled problem (6), (45).

The proof of convergence is similar to and actually simpler than the proof of Section 3.2.4. There are no optimality conditions (25), (29) and hence no estimate (36). The law of decrease for the pseudo-energy is still given by (37):

$$E^{n+1} = E^n - \lambda \sum_k \left(\int_{\Omega_k} |eu_k^n + 1|^2 + |eu_k^n|^2 \, dx \right).$$

4. SOLVING OTHER PROBLEMS

4.1. The Inhomogeneous Case

Now we come back to the inhomogeneous problem (1) with non-constant coefficients μ and ρ. These coefficients and their first derivatives are supposed to be piecewise continuous, so that the problem is well posed.

We modify the domain decomposition algorithm as follows,

$$\begin{cases} -\nabla(\mu_k \vec{\nabla} u_k^{n+1}) - \omega^2 \rho k u_k^{n+1} = 0 & \text{in } \Omega_k \\ \mu_k \dfrac{\partial}{\partial \nu_k} u_k^{n+1} + i\beta_k \omega u_k^{n+1} = -\mu_j \dfrac{\partial}{\partial \nu_j} u_j^n + i\beta_j \omega u_j^n & \text{on } \Sigma_{kj} \\ \mu_k \dfrac{\partial}{\partial \nu_k} u_k^{n+1} + i\beta_k \omega u_k^{n+1} = 0 & \text{on } \Gamma_{k,\text{ext}} \\ \dfrac{\partial}{\partial \nu_k} u_k^{n+1} = \dfrac{\partial}{\partial \nu_k} u_{\text{inc}} & \text{on } \Gamma_{k,\text{int}}, \end{cases} \tag{46}$$

where μ_k denotes the value of μ in Ω_k. We necessarily have $\mu_k = \mu_j$ on Σ_{kj}. The (β_k) are real positive coefficients to be determined. They must satisfy $\beta_k = \beta_j$.

A study of the dimensionality of these equations indicates that β has to be of the same dimension as $\sqrt{\mu\rho}$. A possible choice for β_k (and β_j) on Σ_{kj} is

$$\beta_k = \frac{1}{2}(\sqrt{\mu_k \rho_k} + \sqrt{\mu_j \rho_j}),$$

the arithmetic mean value of $\sqrt{\mu_k \rho_k}$ on the interface.

The pseudo-energy has to be modified accordingly:

$$\begin{aligned} E^n = {} & \sum_{k \neq j} \int_{\Sigma_{kj}} \left(\frac{1}{\beta_k} \left| \mu_k \frac{\partial}{\partial \nu_k} eu_k^n \right|^2 + \beta_k \omega^2 |eu_k^n|^2 \right) d\sigma \\ & + \sum_k \int_{\partial\Gamma_{k,\text{ext}}} \left(\frac{1}{\beta_k} \left| \mu \frac{\partial}{\partial \nu_k} eu_k^n \right|^2 + \beta_k \omega^2 |eu_k^n|^2 \right) d\sigma. \end{aligned} \tag{47}$$

The proof of convergence now follows the same steps as in Section 2.

The optimal control case generalizes likewise to the inhomogeneous case.

4.2. Other Boundary Conditions

We already pointed out the importance of the lowest order absorbing condition in the convergence process (Section 2.2.3). This section shows how to deal with different boundary conditions.

4.2.1. *Waveguide Transparent Condition*

We present here a wave guide problem which involves a non-local transparent boundary condition. For more details and comments on this formulation and more general cases see [21, 25, 27, 28, 35]. The wave guide is made of

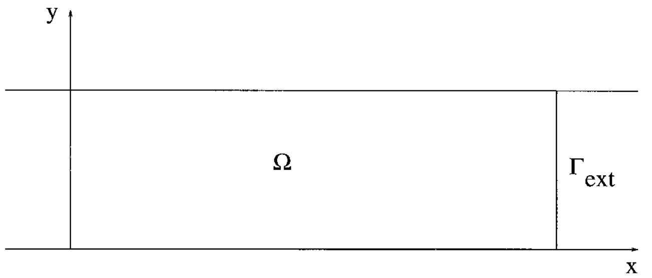

FIG. 8. A wave guide.

an infinite 2-D strip Ω defined by $0 < y < L$ in a space described with Cartesian coordinate (x, y) (see Fig. 8).

If we consider the homogeneous Helmholtz equation (6) inside Ω and Neumann boundary conditions $(\partial/\partial y)u = 0$ on $y = 0, L$, the solution u can be decomposed on an infinite number of modes. More precisely, we write

$$u(x, y) = \sum_{l=0,\infty} \hat{u}_l(x) \cos\left(\frac{l\pi}{L} y\right).$$

The lth mode $\hat{u}_l$ satisfies the 1-D Helmholtz equation (we normalize L to 1 for simplicity),

$$-\frac{\partial^2}{\partial x^2}\hat{u}_l + (l^2\pi^2 - \omega^2)\hat{u}_l = 0, \tag{48}$$

for which an exact analytic solution can be derived.

If we decide to close the exit of the wave guide (on the side $x > 0$) with a transparent boundary Γ_{ext} (see Fig. 8), we can derive an exact transparent boundary condition mode by mode. We have two possibilities:

First, if $l\pi < \omega$, the mode is propagative. We know the exact form of the outgoing solution of (48). It satisfies

$$\frac{\partial}{\partial x}\hat{u}_l + i\sqrt{\omega^2 - l^2\pi^2}\,\hat{u}_l = 0 \quad \text{on } \Gamma_{\text{ext}}. \tag{49}$$

Second, if $l\pi > \omega$, the mode is evanescent and the boundary condition is

$$\frac{\partial}{\partial x}\hat{u}_l + \sqrt{l^2\pi^2 - \omega^2}\,\hat{u}_l = 0 \quad \text{on } \Gamma_{\text{ext}}. \tag{50}$$

An analogous transparent boundary condition can be defined as the $x < 0$ side. If we decide to decompose the waveguide in successive slices in x (Fig. 9), we can try to apply the domain decomposition method (Section 2) on this example.

The modal decomposition of the transmission condition (see (11)) is

$$\frac{\partial}{\partial x}\hat{u}_{l,k}^{n+1} + i\omega\hat{u}_{l,k}^{n+1} = \frac{\partial}{\partial x}\hat{u}_{l,j}^{n} + i\omega\hat{u}_{l,j}^{n} \quad \text{on } \Sigma_{kj}.$$

We immediately see in the proof of convergence that the boundary condition (49) for propagative modes will induce no problems as this boundary condition has the form of a first order absorbing boundary condition. The corresponding pseudo-energy for the lth mode indeed satisfies the decrease law

$$\hat{E}_l^{n+1} = \hat{E}_l^n - 2\omega^2 \sum_k \int_{\Gamma_{k,\text{ext}}} |\hat{e}_{l,k}^{n+1}|^2 + |\hat{e}_{l,k}^n|^2\, d\sigma.$$

Conversely, for the evanescent modes and because of the real coefficient $\sqrt{l^2\pi^2 - \omega^2}$ in (50), the pseudo-energy is stationary:

$$\hat{E}_l^{n+1} = \hat{E}_l^n.$$

The standard domain decomposition of Section 2 does not converge for evanescent modes. The variants of the algorithm described in the previous section can resolve this problem.

If we use an under-relaxed transmission condition (Section 4.1), i.e.,

$$\frac{\partial}{\partial \omega_k}\hat{u}_{l,k}^{n+1} + i\omega\hat{u}_{l,k}^{n+1} = (1 - r)\left(-\frac{\partial}{\partial \nu_j}\hat{u}_{l,j}^n + i\omega\hat{u}_{l,j}^n\right) + r\left(\frac{\partial}{\partial \nu_k}\hat{u}_{l,k}^n + i\omega\hat{u}_{l,k}^n\right),$$

the decrease law for the pseudo-energy of the evanescent mode $\hat{E}_l^n$ is a modification of (18):

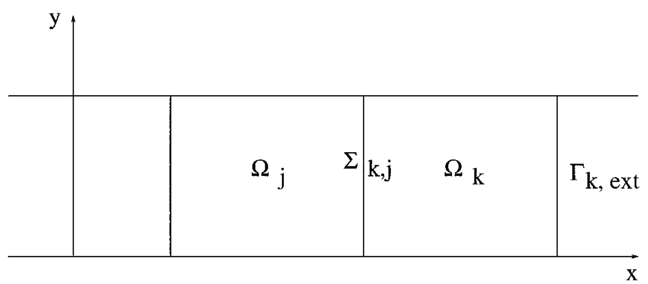

FIG. 9. Decomposition of the wave guide.

$$\hat{E}_l^{n+1} = \hat{E}_l^n - 2r(1-r)\left(\sum_{k,j}\int_{\Sigma_{kj}}\left|\frac{\partial}{\partial\nu_k}\hat{e}_{l,k}^n + \frac{\partial}{\partial\nu_j}\hat{e}_{l,j}^n\right|^2 + \omega^2|\hat{e}_{l,k}^n - \hat{e}_{l,j}^n|^2\,d\sigma\right).$$

There are no terms supported by Γ_{ext} because of the evanescent boundary condition (50) but the additional terms induced by the under-relaxation guarantee convergence.

We can also use the "optimal control" variant of Section 4.1. The fictive adjoint sub-problem associated to (48) (50) is (the problem is actually self-adjoint)

$$-\frac{\partial^2}{\partial x^2}\hat{p}_{l,k}^{n+1} + (l^2\pi^2 - \omega^2)\hat{p}_{l,k}^{n+1} = \hat{u}_{l,k}^{n+1} \quad \text{on } \Omega_k, \tag{51}$$

$$\frac{\partial}{\partial x}\hat{p}_{l,k}^{n+1} + \sqrt{l^2\pi^2 - \omega^2}\,p_{l,k}^{\hat{n}+1} = 0 \quad \text{on } \Gamma_{\text{ext}}. \tag{52}$$

We then add the modal decomposition of the coupled transmission conditions (30):

$$\frac{\partial}{\partial\nu_k}\hat{u}_{l,k}^{n+1} + \lambda\hat{p}_{l,k}^{n+1} = -\frac{\partial}{\partial\nu_j}\hat{u}_{l,j}^n + \lambda\hat{p}_{l,j}^n \quad \text{on } \Sigma_{kj},$$

$$\frac{\partial}{\partial\nu_k}\hat{p}_{l,k}^{n+1} - \lambda\hat{u}_{l,k}^{n+1} = -\frac{\partial}{\partial\nu_j}\hat{p}_{l,j}^n - \lambda\hat{u}_{l,j}^n \quad \text{on } \sigma_{kj}.$$

This procedure converges as outlined in Section 4.2 and the decrease of the pseudo-energy, defined as

$$\hat{E}_l^{n+1} = \sum_{k\neq j}\int_{\Sigma_{kj}}\left|\frac{\partial}{\partial\nu_k}\hat{e}u_{l,k}^{n+1}\right|^2 + \lambda^2|\hat{e}u_{l,k}^{n+1}|^2 + \left|\frac{\partial}{\partial\nu_k}\hat{e}p_{l,k}^{n+1}\right|^2 + \lambda^2|\hat{e}p_{l,k}^{n+1}|^2\,d\sigma,$$

is given by (38).

The introduction of a fictive adjoint problem makes it possible to deal with the embarrassing terms on the boundary (as well as the non-coercive terms in the Helmholtz equation) and to add a coercive term on the right hand side of (51) which will guarantee the decrease of the pseudo-energy and hence the convergence.

4.2.2. *PML Absorbing Layers*

In the case of PML (5) the damping layer replaces in some sense the absorbing boundary conditions. Let us note that, in contrast to classical absorbing boundary conditions, it seems not easy to prove existence of a solution to the system with PML layers (see [11] on this problem). So in this section we simply postulate the existence of the solution with a PML layer.

We now go a bit faster and simply examine the behavior of the algorithm on sub-domains consisting of infinite vertical stripes. This will formally be enough to point out convergence failures and possible cures.

The sub-domains are infinite stripes in the x direction. The interfaces Σ_kj are now lines of equations $x =$ constant. We assume that d is constant on the sub-domains contained in the absorbing layer. For such a sub-domain the pseudo-energy has to be modified (as in the inhomogeneous case) and uses terms of the form

$$\int_{\Sigma_{kj}}\left(\left|d\frac{\partial}{\partial y}eu_k^n\right|^2 + \omega^2|eu_k^n|^2\right)d\sigma.$$

The key point of the demonstration (Section 2.2.3) with the simple transmission condition (see (11)) is to evaluate the cross products

$$\operatorname{Re}\left(\int_{\partial\Omega_k} d\frac{\partial}{\partial\nu_k}eu_k^{n+1}\overline{i\omega eu_k^{n+1}}\,d\sigma\right)$$

which express the quantity by which the pseudo-energy decreases. We integrate by parts an equation of the type (5) for the error and obtain an equivalent of (14):

$$\operatorname{Re}\left(\int_{\partial\Omega_k} d\frac{\partial}{\partial\nu_k}eu_k^{n+1}\overline{i\omega eu_k^{n+1}}\,d\sigma\right) = \operatorname{Re}\left(-i\omega\left(\int_{\Omega_k}\frac{1}{d}\left|\frac{\partial}{\partial x}eu_k^{n+1}\right|^2 + d\left|\frac{\partial}{\partial y}eu_k^{n+1}\right|^2 - \frac{\omega^2}{d}|eu_k^{n+1}|^2\right)dx\right).$$

In (14) the right hand side was vanishing. Now d is a complex number and we immediately see that the real parts in these different coefficients are going to be of opposite sign.

It is therefore not possible to prove the convergence of the classical domain decomposition method. Nor does it seem trivial to use an under-relaxed variant of the algorithm or more general transmission conditions with an arbitrary complex parameter instead of the pure imaginary $i\omega$. Conversely, the optimal control algorithm can solve the problem.

As in Section 5.2.1, we define a fictive adjoint of Eq. (5). As d is a complex parameter, we consider

$$-\partial_{xx}^2 p - \bar{d}\partial_y(\bar{d}\partial_y p) - \omega^2 p = u; \tag{53}$$

then the domain decomposition described in Section 4.2 is easily applied to solve (5), (53) and the proof of convergence gives the same law of decrease for the pseudo-energy.

5. NUMERICAL RESOLUTION

In the framework of the domain decomposition method, various strategies are possible with regard to the shape and number of sub-domains and the discretization and method of resolution of the sub-problems. It is possible to work on a discrete formulation of the global problem. Mixed hybrid finite elements (see [22, 34] on this technique) are for instance well suited to our algorithm for its uses in particular, as degrees of freedom, the fluxes of the normal derivative and the average values of the trace of the direct and adjoint states on the interfaces which are the natural unknowns of our transmission conditions. It allows in particular a direct transcription of the domain decomposition algorithm and the proof of its convergence to the discrete formulation.

We illustrate this paper by the resolution of the direct problem (6) and the corresponding optimal control problem minimizing the cost function (23) reformulated in Section 3.1 as the coupled system (6), (21), (24), (25). For both problems u_{inc} is chosen to be an incident horizontal plane wave. More precisely, we take $u_{\text{inc}} = e^{-i\omega x.\mathbf{h}}$, where $\mathbf{h}$ is the horizontal direction pointing inside the resonator in Fig. 1.

In this experiment, we impose no constraint on the control v. In practice, this means that (25) can be reduced to $v = p/\alpha$ on Γ_{cont} and then used to replace v in (21). The same simplification holds for (29) in the domain decomposition algorithm. The domain decomposition methods now simply amounts to the iterative resolution of the local coupled sub-problems (27) (28) where v_k^{n+1} has been replaced by $-p_k^{n+1}/\alpha$.

The domain Ω is a disk of radius 1. It is discretized (in polar coordinates (r, θ)) using 64×256 mixed hybrid first order finite elements. The resonator is located between discretization levels 40 and 44 in r and has an opening of 16 levels of discretization in θ. We took $\omega = 2\pi \times 6.4$, which roughly corresponds to a 0.16 wavelength. The numerical parameter λ in the transmission conditions (30) is set to $\lambda = \omega$. The penalization parameter α in (23) is set to $\alpha = 1/\omega^3$ for dimensional reasons.

Each finite element is taken to be a sub-domain of the domain decomposition method. Then, each local solution involves a small number of degree of freedoms and can be computed analytically as a function of the second hand terms of the transmission conditions (30) which are given by the neighboring sub-problems at the previous iteration. The algorithm reduces to explicit formulae and transmission of data between sub-domains.

For more on the massively parallel strategy (implemented on a Connection Machine) see [2, 3]. See also [18] for a coarser decomposition combined with a local conjugate gradient resolution implemented on the T3D to solve 3-D Maxwell direct problems.

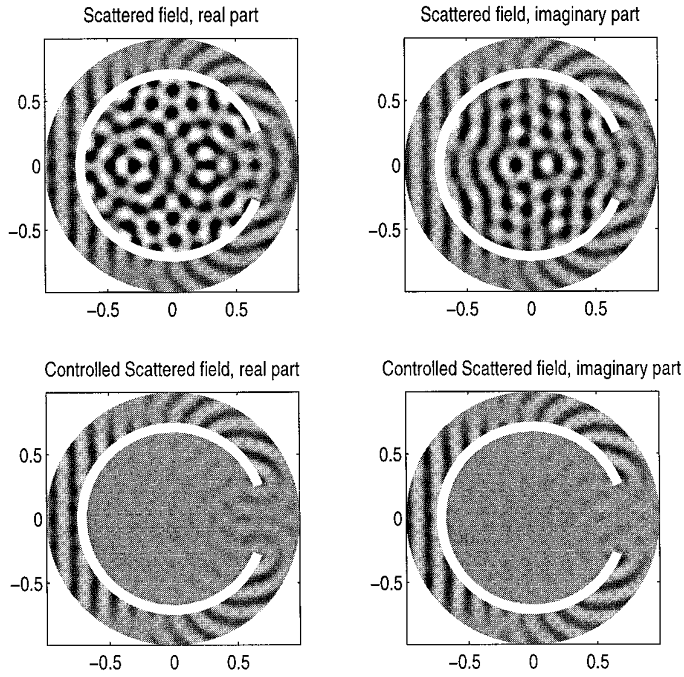

FIG. 10. Scattered field, in which a plane wave arrives from the right.

We now comment on the results displayed in Fig. 10, which give a qualitative indication of the ability of this algorithm to compute direct and optimal control problem for the Helmholtz equation. A plane wave arrives from the right and we display the scattered field. At the top of Fig. 10, there is no control; we see the multiple reflections caused by the hard resonator. At the bottom we see the optimal control solution generated by our algorithm. Reflections are killed inside but not outside as the control only acts on the inside boundary of the resonator.

REFERENCES

1. A. Bayliss and E. Turkel, Radiation boundary conditions for wave like equations, *Comm. Pure Appl. Math.* **33,** 707 (1980).
2. J. D. Benamou, A domain decomposition method for the optimal control of system governed by the Helmholtz equation, in *Third International Conference on Mathematical and Numerical Wave Propagation Phenomena* (*Cannes–Mandelieu*), edited by G. Cohen (SIAM, Philadelphia, 1995), p. 653.
3. J. D. Benamou, A massively parallel algorithm for the optimal control of systems governed by elliptic p.d.e.'s, in *Seventh SIAM Conference on Parallel Processing for Scientific Computing, San Francisco* (SIAM, Philadelphia, 1995).
4. J. D. Benamou, Domain decomposition methods with coupled transmission conditions for the optimal control of systems governed by elliptic partial differential equations, *SIAM J. Numer. Anal.* **33** (1996).
5. J. Berenger, A perfectly matched layer for the absorption of electromagnetic waves, *J. Comp. Phys.* **114,** 185 (1994).
6. D. Bouche and F. Molinet, *Méthodes asymptotiques en électromagnétisme* (Masson, Paris, 1989).

7. X.-C. Cai and O. B. Widlund, Domain decomposition algorithm for indefinite elliptic problems, *Siam J. Sci. Stat. Comput.* **13,** 243 (1992).
8. X.-C. Cai and O. B. Widlund, Multiplicative algorithms for some nonsymmetric and indefinite problems, *SIAM J. Numer. Anal.* **30,** 936 (1993).
9. O. Cessenat and B. Despres, *Une nouvelle formulation variationnelle des équations d'ondes en fréquence. Application au problème de Helmholtz 2d,* Technical Report 2779 (CEA, 1994).
10. F. Collino, Perfectly matched absorbing layers for the paraxial equations, *J. Comp Phys.,* to appear.
11. F. Collino and P. Monk, The perfectly matched layer in curvilinear coordinates, *SIAM J. Sci. Comput.,* to appear.
12. D. Colton and R. Kress, *Integral Equation Method in Scattering* (Wiley–Interscience, New York, 1983).
13. C. Colton and R. Kress, *Inverse Acoustic and Electromagetic Scattering Theory* (Springer-Verlag, Berlin/New York, 1992).
14. A. de la Bourdonnaye, *A Substructuring Method for a Harmonic Wave Propagating Problem: Analysis of the Conditioning Number of the Problem on the Interfaces,* Technical Report 95-35 (CERMICS, 1995).
15. B. Després, *Méthodes de décomposition de domaine pour les problèmes de propagation d'ondes en régimes harmoniques,* Ph.D. thesis (Paris 9 France, 1991).
16. B. Després, Domain decomposition method and the Helmholtz problem, ii, in *Second International Conference on Mathematical and Numerical Aspects of Wave Propagation Phenomena,* edited by R. Kleinman, T. Angell, D. Colton, F. Santosa, and I. Stackgold, (SIAM, Philadelphia, 1993), p. 197.
17. B. Després, P. Joly, and J. E. Roberts, A domain decomposition method for the harmonic Maxwell's equations, in *IMACS International Symposium on Iterative Methods in Linear Algebra,* edited by R. Beauwens and P. de Groen, (North-Holland, Amsterdam, 1992), p. 475.
18. Bruno Despres, Implementation of a non overlapping domain decomposition method on a Cray t3d, for solving the 3d harmonic Maxwell's equations, in *International Symposium on Maxwell's Equations* (IMA, 1994).
19. J. Douglas, P. J. Paes Leme, J. E. Roberts, and J. Wang, A parallel iterative procedure applicable to the approximate solution of second order partial differential equations by mixed finite element methods, *Numer. Math.* **65,** 95 (1993).
20. O. Ernst and G. Golub, A domain decomopsition approach to solving the Helmholtz equation with a radiation boundary condition, in *Domain Decomposition Methods in Science and Engineering,* edited by A. Quarteroni, J. Periaux, Y. Kuznetsov, and O. Widlund (Amer. Math. Soc., Providence, RI, 1992), p. 177.
21. G. J. Fix and S. P. Marine, Variational methods for underwater acoustic problems, *J. Comp. Phys.* **28,** 253 (1978).
22. J. E. Roberts and G. Chavent, A unified physical presentation of mixed, mixed-hybrid finite elements and usual finite differences for the determination of velocities in waterflow problems, *Adv. Water Resources* **14,** 329 (1991).
23. J. Paoli, G. Roge, and C. Bardos, Maîtrise du champ rétrodiffusé par une méthode de contrôle optimal [*Preprint*].
24. D. Givoli, Non reflecting boundary conditions, *J. Comp. Phys.* **94,** 1 (1991).
25. D. Givoli and J. B. Keller, Exact nonreflecting boundary conditions, *J. Comp. Phys.* **82,** 172 (1989).
26. C. I. Goldstein, The finite element method with non uniform mesh sizes applied to the exterior Helmholtz problem, *Numer. Math.* **38,** 61 (1981).
27. C. I. Goldstein, A finite element method for solving Helmholtz type equations in wave guides and other unbounded domains, *Math. Comp.* **39,** 309 (1982).
28. T. Hagstrom and H. B. Keller, Asymptotic boundary conditions and numerical methods for non linear elliptic problems in unbounded domains, *Math. Comput.* **48,** 449 (1987).
29. J. E. Santos, J. Douglas, and F. Pereira, A parallelizable approach to the simulation of waves in dispersive media, in *Third International Conference on Mathematical and Numerical Wave Propagation Phenomena* (*Cannes–Mandelieu*), edited by G. Cohen (SIAM, Philadelphia, 1995), p. 673.
30. J. L. Lions, *Contrôlabilité exacte perturbations et stabilisation de systèmes distribués,* tome 1 (Masson, Paris, 1988).
31. P. L. Lions, On the Schwarz alternating method, 3, in *Third International Symposium on Domain Decomposition Methods for Partial Differential Equations,* edited by T. F. Chan, R. Glowinski, J. Périaux, and O. B. Widlund (SIAM, Philadelphia, 1990), p. 202.
32. P. Joly, M. Invernizzi, F. Collino, and A. Piacentini, A new transmission operator in the domain decomposition for the maxwell equations, in *ECNUM* (1995).
33. J. C. Nedelec, Curved finite element methods for the solution of singular integral equations on surfaces on R^n, *Comp. Methods Appl. Mech. Engrg.* **8,** 61 (1971).
34. J. C. Nedelec, A new family of mixed finite elements in r^3, *Numer. Math.* **50,** 57 (1986).
35. C. Poirier and P. Joly, Mathematical analysis of electromagnetic open waveguides, *M2AN* **29,** 505 (1995).
36. J. L. Lions and R. Dautray, *Analyse mathématique et calcul numérique pour les sciences et techniques,* tome 1 (Masson, Paris, 1985).
37. C. M. Rappaport, Perfectly matched absorbing boundary conditions based on anisotropic lossy mapping of space, *IEEE Microwave Guided Wave Lett.* **5** (1995).
38. P. Joly, S. Ghanemi, and F. Collino, Domain decomposition method for harmonic wave equations, in G. Cohen, editor, *Third International Conference on Mathematical and Numerical Wave Propagation Phenomena* (*Cannes–Mandelieu*), edited by G. Cohen (SIAM, Philadelphia, 1995), p. 663.
39. J. A. Stratton, *Electromagnetic Theory* (McGraw-Hill, New York, 1941).
40. E. I. Ogorodnikov and V. V. Shaidurov, Some numerical method of solving Helmholtz wave equation, in *Mathematical and Numerical Aspects of Wave Propagation Phenomena,* (SIAM, Philadelphia, 1991), p. 73.